Aperture-Array Directional Sensing using 2-D Beam Digital Filters with Doppler-Radar Front-Ends

Tharindu Randeny, Arjuna Madanayake and Arindam Sengupta
Department of Electrical and Computer Engineering (ECE),
The University of Akron,
Akron, Ohio, USA.
Email: arjuna@uakron.edu,{tdr40,as206}@zips.uakron.edu

Yiran Li and Changzhi Li
Department of ECE,
Texas Tech University,
1012 Boston Avenue, Lubbock, TX, 79409.
Email: changzhi.li@ttu.edu

***Abstract*—A directional sensing algorithm is proposed employing doppler radar and low-complexity 2-D IIR spatially bandpass filters. The speed of the scatterer is determined by the frequency shift of the received signal following down-conversion. The downconversion is done by mixing it with the instantaneous transmitted signal. The direction of the scatterer is determined by the means of 2-D plane-wave spectral characteristics, using 2-D IIR beam filters. The proposed architecture was simulated for three scatterers at 10,^{o} 30,^{o} 60^o from array broadside, traveling at speeds of 31 ms,$^{-1}$ 18 ms^{-1} and 27 ms^{-1}, respectively. A doppler radar module was used to transmit and receive reflected signals, that has a carrier frequency of 2.4 GHz. Simulations show both direction and doppler information being enhanced.**

***Keywords*—Multidimensional signal processing, directional sensing, 2-D IIR digital filters, doppler, radar, cyberphysical systems.**

I. Introduction

Radio frequency (RF) sensing using a uniform linear array (ULA) aperture is important for radar applications. Beamsteering antennas, when combined with doppler radar, leads to an electronically-steerable directional RF sensor that can obtain radar signatures from moving targets.

In addition to range, direction and velocity, radar can lead to microwave imaging and other remote sensing applications. Radars with direction, range and doppler information are finding new applications in cyberphysical systems (CPS). For example, autonomous vehicles (AV) including but not limited to self-driving cars, package delivery drones, airborne wireless basestations and defense/intelligence systems need RF sensors. Emphasis has been placed upon ensuring real-time systems for AVs in order to avoid collisions and other situational awareness [1]. Directional RF sensing thus plays an important role as a sensing modality among a multitude of modalities, such as video and infrared cameras, LIDAR and ultrasonic sensors, which continuously provide situational awareness data to the AV's control system, through sensor fusion algorithms. In this paper, we propose the joint application of doppler radar to recently proposed two-dimensional 2-D recursive digital beam filters, to obtain the proposed low-complexity electronically-steerable directional doppler-radar sensor for linear aperture array. Fig. 1 shows a typical application of the proposed architecture in automotive CPS, where the velocities of moving objects lead to detectable doppler signatures.

Continuous-wave doppler radars have recently been used to measure velocity of radar targets, remote tracking, health monitoring, and motion-adaptive therapeutics [2]–[8]. However, obtaining positional details using doppler radar sensors require digital phased-array beamforming architectures that lead to complex electronic systems [9]–[12]. Such systems, when realized using reconfigurable digital logic fabrics, such as field-programmable gate arrays (FPGAs), result in high resource and power consumptions. Phased-array receivers have well-known limitations on the maximum detectable range, associated with the targets in motion. Introduction of 2-D IIR beam filters, on the other hand, offer comparable directional selectivity albeit at a lower arithmetic complexity when compared to FFT-based digital phased-array receivers having similar directivity [13]. Thus, replacing FFT-based phased-arrays with 2-D digital beamfilter based steerable apertures reduces the overall complexity of the digital architecture. In this paper, we introduce a methodology that integrates doppler radars with array signal processing based on 2-D infinite impulse response (IIR) spatial bandpass (SBP) beam digital filters [14]–[16], in order to sense the direction of arrival (DOA) and velocity of moving objects.

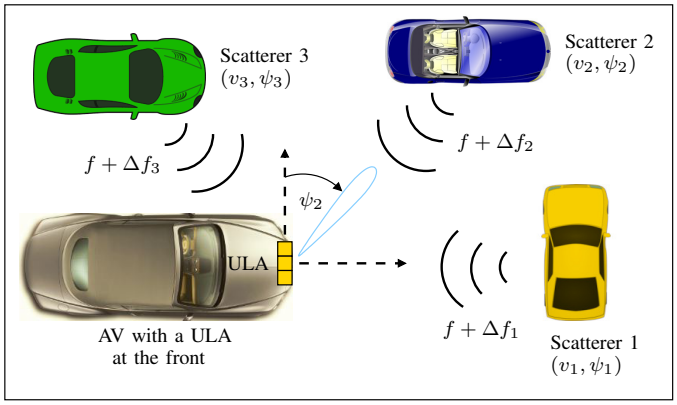

Fig. 1. A typical application of the proposed architecture in the field of cyberphysical systems.

II. Doppler 2-D IIR SBP Beam Architecture

The moving objects in the neighborhood of the doppler radar are tracked in 2-D spatio-temporal (ST) domain as a function of (i) velocity (speed and direction), (ii) broadside angle with respect to the ULA of receiver antennas and range, measured from the center of the ULA. Doppler radar achieves speed measurement via the frequency shift introduced by moving targets in the radio environment. The direction of the moving targets can be determined by using a ULA

978-1-4799-1740-2/15/$31.00

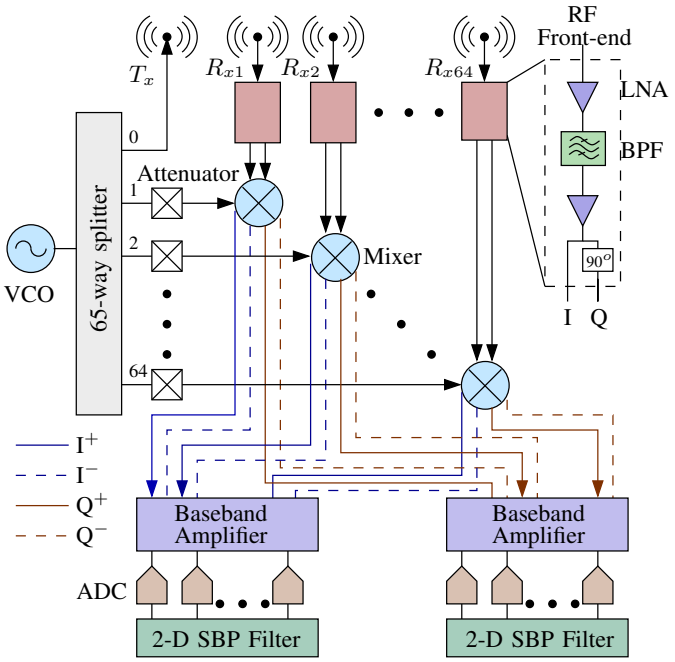

Fig. 2. Overview of the proposed architecture. The transmit antenna sends out a signal S_T, and the reflected signal S_R is received using a ULA of antennas, where the velocities and directions of the moving objects is detected, following several stages of signal processing.

of receiver antennas, that offers electronic steerability, using multi-dimensional signal processing techniques.

Fig. 2 shows an overview of the proposed doppler 2-D SBP beam sensing sensor. The radar design consists of a wideband omnidirectional antenna, T_x, for transmitting a signal S_T. The outgoing wave strikes surrounding moving objects. A ULA of 64 receiver antennas, R_{x1}, R_{x2} $\cdots$ R_{x64}, will spatially sample the reflected RF waves S_R. The spacing between antennas is set as $\Delta x = \lambda_{min}/2$, where λ_{min} corresponds to the shortest wavelength of the received signals (i.e., for the highest frequency component). Each receiver antenna feeds its own RF front-end, which consists of a low noise amplifier (LNA), a band-pass filter (BPF), a gain ampliflier (GA), and a phase-shifter, giving rise to in-phase (I) and quadrature (Q) components of the received signals. The signals are then subjected to mixing, for downconverting the received signals to baseband frequencies (BFs). Down-conversion is achieved by multiplying the outputs from the receiver with a copy of the transmit signal S_T, using a voltage-controlled oscillator (VCO) and a 65-way splitter. The downconverter output is followed by a baseband amplification stage and a low-pass filtering operation for image rejection.

The speed of the moving target is proportional to the frequency of the downconverted signal. The downconverted signals are then downsampled using a dedicated downsampling analog-to-digital converters (ADCs), at each antenna stage. The reflected signal obtained using the ULA yields a 2-D discrete domain ST sequence $w_{RF}(n_x, n_{ct})$, where $n_x = 0, 1, \cdots, 63$ is the antenna index, and $n_{ct} = 0, 1, \cdots, N_{ct} - 1$ is the time sample index, where N_{ct} corresponds to the number of samples. *The received sequence $w_{RF}(n_x, n_{ct})$ after the downsampling stage, is then digitally processed using the 2-D IIR SBP beamformer, to determine the direction-of-arrival (DOA) of the signal, thereby providing the angular information of the surrounding targets.*

A. Doppler Radar

The choice of continuous wave (CW) radar arises due to its ability to use narrowband chirped signals, unlike pulse radars, thereby reducing the bandwidth requirements. The relative movement between the ULA and targets gives rise to the doppler shift in the received frequency, as a result of the change in distance between adjacent wavefronts of S_T and S_R. The relationship between target-speed and the received RF is given by [17], [18]

$$f_r = \left(\frac{c + v_r}{c - v_s}\right) f_c \tag{1}$$

where f_r and f_c denote the received and transmitted frequencies, v_r and v_s are target and source speeds and $c \approx 3 \cdot 10^8 ms^{-1}$ is the speed of light, respectively. Once the received signal is downconverted (by mixing the received signal with the transmitted signal) the multi-dimensional spectrum shows the temporal frequency shift (Δf) between the two signals, which corresponds to the relative velocity of the object, assuming $c >> v$, as expressed by [17], [18]

$$v = \frac{\Delta f c}{f_c} \tag{2}$$

By introducing a chirp mode signal with linearly varying frequency we can detect the range profiles of the scatterers in the neighbourhood. Since the frequency is swept linearly, it results in the down converted signal containing an intermediate frequency corresponding to the frequency shift between the transmitted and received signal, which is directly proportional to the range of the scatterer. The frequency shift of the chirped mode signal used to detect the range profiles (R_s) of static scatterers expressed by the relation [18], [19]

$$R_s = \Delta f \left(\frac{T_s}{B}\right) c \tag{3}$$

where T_s and B represent the sweep time and the bandwidth, of the chirp radar system, respectively.

B. 2-D IIR SBP Filter

A far field propagating plane wave (PW) signal w_t in the 3-D space $(x, y, z) \in \mathbb{R}^3$ can be approximated by a 4-D spatio-temporal (ST) planar wave signal $w(x, y, z, ct)$ given by [20]

$$w(x, y, z, ct) = w_t(d_x x + d_y y + d_z z + ct) \tag{4}$$

where d = $[d_x\ d_y\ d_z]$ is the unit vector specifying the direction of arrival (DOA) and ct denotes time t scaled by the speed of light c.When such 4-D ST PW signals are received by a ULA of antennas comprising of N elements spaced Δx apart such that Δx satisfies the spatial Nyquist sampling condition (i.e $\Delta x = \lambda_{min}/2$), 4-D ST PW further reduces to a 2-D ST PW [21] given by

$$w(x, ct) = w_t(d_x x + ct) \tag{5}$$

The directional vector d_x relates to the spatial DOA of the signal, defined as the angle between normal to the wavefront and the normal to the array, and is represented as ψ. Time synchronous sampling of the 2-D spatio-temporal planar wave

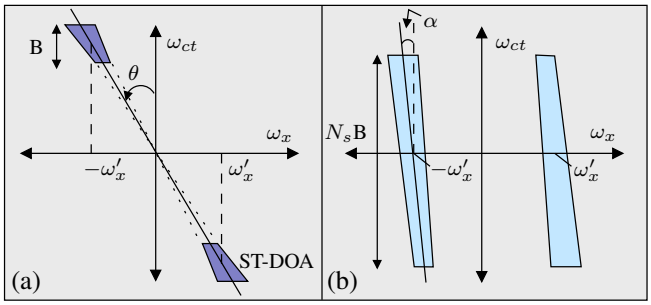

Fig. 3. (a)The ROS of 2-D plane-waves, arriving at a spatio-temporal DOA θ, assumes a trapezoidal shape; (b) The 2-D spectrum after downconversion, and downsampling by a factor N_s, inclined at an angle α, centred about $\pm\omega'_x$. We note that the spatial frequency index (ω_x) in (a) and (b) remain the same.

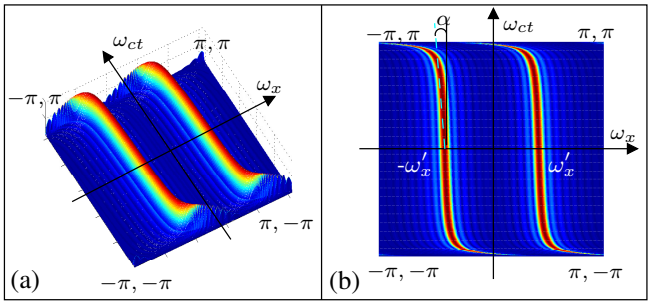

Fig. 4. (a) Magnitude response of the 2-D IIR SBP filter; (b) Top view of the 2-D response with passband inclined at an angle α, centered about $\pm\omega'_x$.

at a sampling frequency F_s using N analog to digital converters (ADCs) lead to the 2-D discrete domain ST sequence $w(n_x, n_{ct})$ where $n_x = 0, 1, \cdots, N-1$ is the antenna index, and $n_{ct} = 0, 1, \cdots, N_s - 1$ is the time sample index. The frequency domain representation of $w(n_x, n_{ct})$ is obtained by following the 2-D discrete Fourier transform (DFT) and the region of support (ROS) of the PW spectrum in the (ω_x, ω_{ct}) domain is a straight line passing through the origin [22]:

$$\omega_x - \omega_{ct} \sin\psi = 0 \tag{6}$$

Fig. 3(a) shows the ROS of the received signal w_t. In order to selectively enhance broadband PWs depending on their DOAs, a 2-D IIR frequency planar filter can be implemented by aligning the ROS of the filter with that of the desired spatio-temporal planar wave DOA [21]. The transfer function (TF) of a 2-D IIR frequency-planar beam filter based on a first-order resistively terminated passive network [21] which are practical bounded-input-bounded-output (P-BIBO)stable [23]:

$$H(z_1, z_2) = \frac{(1 + z_1^{-1})(1 + z_2^{-1})}{1 + b'_{10} z_1^{-1} + b'_{01} z_2^{-1} + b'_{11} z_1^{-1} z_2^{-1}} \tag{7}$$

where, b'_{ij} are the ST feedback coefficients, given by

$$b'_{ij} = \frac{R + (-1)^i \frac{2\cos\theta}{\Delta x} + (-1)^j \frac{2c\sin\theta}{\Delta T}}{R + \frac{2\cos\theta}{\Delta x} + \frac{2c\sin\theta}{\Delta T}}, i + j \neq 0 \tag{8}$$

In typical wireless systems, RF signals received by each antenna in the ULA are down-converted to baseband or intermediate frequency. In such a scenario where signals are down converted and down sampled with a temporal down sampling factor N_s 2-D spectral properties are changed as shown in Fig. 3(b) [14].It could be seen that the spatio-temporal DOA changes to an angle α with a spatial shift, ω'_x, in the spatial frequency axis.Here, $\alpha = \tan^{-1}\left(\frac{1}{N_s}\sin\psi\right)$ and $\omega'_x = \pm\left(\pi \frac{f_c}{f_c + B}\sin\psi\right)$ [24]. Therefore, the downconverted and down-sampled 2-D signal has ROS at an angle α to the temporal axis, centered along the spatial frequencies $\pm\omega'_x$.The design requirements of the beamforming SBP filter hence must have the passbands centered along the same spatial frequencies $\pm\omega'_x$ in order to selectively enhance the desired spatio-temporal planar wave signal of interest.

The 2-D SBP beam filter is an extension of the 2-D frequency planar beam filters to selectively enhance temporally down-converted and down-sampled (DCDS) spatio-temporal planar wave signals [20], [21], [25]. The 2-D magnitude response of a 2-D IIR frequency planar filter has a passband along the ROS centered along the origin. To construct the passband centering along ω'_x, the 2-D IIR SBP filter can be designed by spatially modulating, i.e., by multiplying the impulse response of the 2-D IIR frequency planar beam filter with $\cos(\omega'_x.n_1)$. The discrete domain transfer function of the 2-D IIR SBP filter is given by [14]–[16]

$$H_{sbp}(z_x, z_{ct}) = \frac{\sum_{i=0}^{2}\sum_{j=0}^{2} a_{ij} {z_x}^{-i} {z_{ct}}^{-j}}{1 + \sum_{i=0}^{2}\sum_{j=0}^{2} b_{ij} {z_x}^{-i} {z_{ct}}^{-j}} (1 + {z_{ct}}^{-1}) \tag{9}$$

where, the coefficients a_{ij} and b_{ij} are formulated in terms of α and ω'_x. The closed form expressions of the coefficients are,

$$\begin{array}{cc}
a_{00} = 1 & b_{00} = 0 \\
a_{01} = b'_{01} & b_{01} = 2b'_{01} \\
a_{02} = 0 & b_{02} = {b'}^2_{01} \\
a_{10} = \cos(\omega'_x)(1 + b'_{10}) & b_{10} = 2b'_{10}\cos(\omega'_x) \\
a_{11} = \cos(\omega'_x)(b'_{01} + b'_{11}) & b_{11} = 2\cos(\omega'_x)(b'_{10}b'_{01} + b'_{11}) \\
a_{12} = 0 & b_{12} = 2b'_{01}b'_{11}\cos(\omega'_x) \\
a_{20} = b'_{10} & b_{20} = {b'}^2_{10} \\
a_{21} = b'_{11} & b_{21} = 2b'_{10}b'_{11} \\
a_{22} = 0 & b_{22} = {b'}^2_{11}
\end{array} \tag{10}$$

where, b'_{ij} are the feedback coefficients, expressed in (8).Fig. 4 shows the magnitude response of the 2-D IIR SBP filter, where the spatial frequency shift of the beam passband is observed.

In this study, the use of doppler radar results in the received signal at RF, denoted as S_R, occupying the low-frequency tone centered at ω'_{ct}, with the ROS inclined corresponding to the DOA. Downconversion of the S_R using S_T results in all the ROS frequencies at RF being mapped to the corresponding frequencies at BF, which is the frequency shift Δf introduced by the relative motion between the target and the ULA receiver aperture. This frequency shift is used to estimate the velocity of the target, with respect to the radar target, because the low-frequency tone is proportional to speed, and the angle is given by the steered-angle of the aperture. The SBP filter can therefore be employed to scan and obtain the value of ω'_x for the desired scatterer ROS, by setting $\alpha = 0$. The term α is set to zero, as the ROS after downconversion, in this case, is a straight line. Once we obtain ω'_x, we can evaluate the DOA ψ using (6). Here, ω'_{ct} is the temporal frequency bin at RF corresponding to $\omega_x = \omega'_x$.

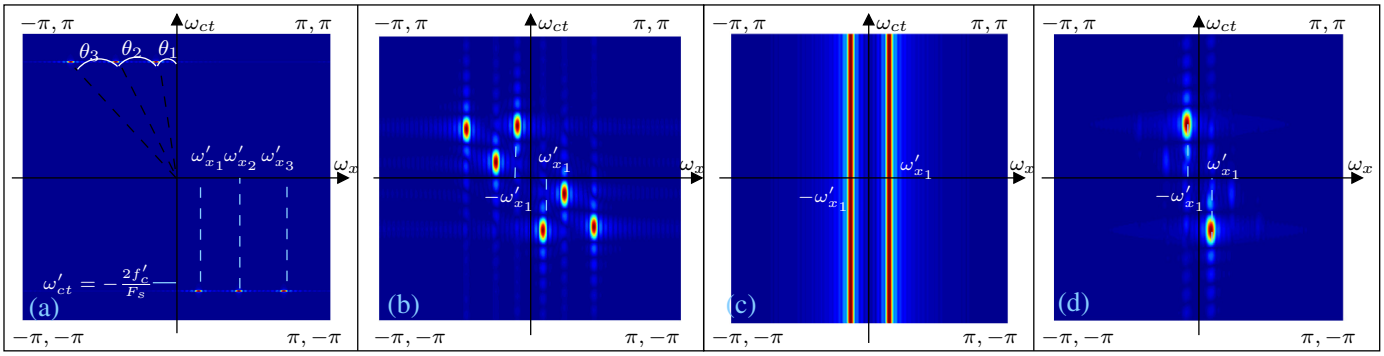

Fig. 5. a) The ROS of reflected signals are inclined at $\theta_k = \tan^{-1}(\sin\psi_k)$, where $\psi_k = 10^o$, 30^o and 60^o for $k \in \{1, 2, 3\}$. The spatial frequencies ω'_{x_i}, for $i \in \{1, 2, 3\}$ are given a temporal frequency ω'_{ct} for the three cases; b) The ROS of the downsampled downconverted signal. The spatial frequency corresponding to the object of interest is shown; c) Frequency response of the 2-D IIR SBP filter with coefficients adjusted to filter out a Doppler-shifted planar wave arriving at an angle of $\psi = 10^o$; d) Directional sensing of the desired target using the 2-D IIR SBP filter having passband centered at $\pm\omega'_{x_1}$.

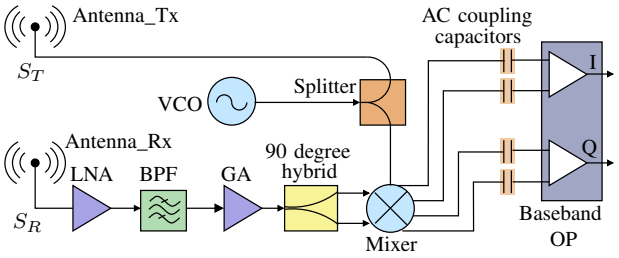

Fig. 6. Block diagram depicting the radar prototype for a single element.

III. RF Front-End and Antenna-Array Design

The doppler-radar RF section has been prototyped using connectorized designs as well as custom-designed RF micro-circuits at the printed circuit board (PCB) level. The front-end is an adaption of the low-cost i-Motion non-directional radar module developed by the authors at Texas Tech [3]. A single element of a doppler module was designed and prototyped at a nominal carrier frequency of 2.4 GHz. Fig. 8 denotes the designed RF PCB. The downconverter is AC-coupled via a differential amplifier stage, to obtain improved common mode rejection. The single element radar module was designed with a direct-conversion radar architecture. Fig. 6 is the simplified block diagram of our single element radar prototype. Both transmitter and receiver chain are shown in the diagram. For the transmitter design, a VCO is adopted to generate a 2.4 GHz carrier signal with a power level around 0 dBm. This VCO also works as the local oscillate (LO) source for the mixer in the receiver chain. A 2.4 GHz carrier signal will be transmitted into air by the antenna on transmitter end.

An LNA, a BPF, a gain block, a balun, a mixer and two baseband operational amplifiers (OPs) forms the receiver chain. The received modulated signal is amplified by the LNA at 2.4 GHz with a 19 dB gain. The BPF after LNA is used to suppress the interferences with frequencies outside the 2.4 GHz band. A gain block with a gain of 12.3 dB is employed to further amplify the received signal. In order to generate two inputs for the downconversion mixer, the amplified signal is divided into two differential signals with a 180-degree phase difference by a balun. The mixer will convert the high frequency signals to baseband signals. The baseband signals are finally amplified by the 40 dB gain baseband OPs. To achieve AC coupling, capacitors are used between the outputs of mixer and inputs of baseband OPs. The supply voltage range for the prototype can vary from 4.8 V to 5.5 V. In on going work, we are in the process of replicating the single element radar receiver that is already prototyped, to 64 elements for directional array processing.

The system uses a single VCO for chirp modulated signals, and the amplifiers and filters are adapted to accomodate the total bandwidth of chirp modulation. Chirping is required to obtain range measurements. In non-chirp mode, the radar can obtain velocity and DOA only. By using multi-modal sensing with chirp, we can obtain speed, DOA and range. The RF-front end will be prototyped using miniature integrate circuits on custom PCB with support for upto 64 elements, and the digital back-end running the 2-D IIR SBP will eventually operate using high-performance micro-controller array or system-on-chip embedded processor with support for 128 low-bandwidth analog inputs.

IV. Simulation Results

To demonstrate the directional sensing capability of the proposed algorithm, we consider three objects surrounding the radar target, moving in at angles $10,^o$ $30,^o$ 60^o with velocities of 31 ms,$^{-1}$ 18 ms^{-1} and 27 ms^{-1}, respectively. We use a simulated doppler radar module placed in the radar target, comprising of a transmit antenna and a ULA of 64 receiver antennas, to transmit and receive reflected signals, that uses a carrier frequency $f_c = 2.4$ GHz. The temporal frequencies are normalized using the sampling frequency $F_s = 5$ GHz. Fig. 5(a) shows the ROS of the set of received signals at various DOAs. The received signals are then downconverted by mixing them with the transmitted signal. Because the downconverted signal has a frequency that is smaller than the original transmitted signal, we downsample the downconverted signal to alleviate the high sampling rate requirement. As shown in Fig. 5(b), it can be seen that the temporal frequency shifts have been spread out (that is, bandwidth expanded) due to the down sampling process.

The DCDS signal is then sent through a 2-D IIR SBP, that can be steered for different angles by appropriately adjusting the filter co-efficients, by varying ω'_x for a fixed ω_{ct} and using (6). By moving the downconversion operation to an

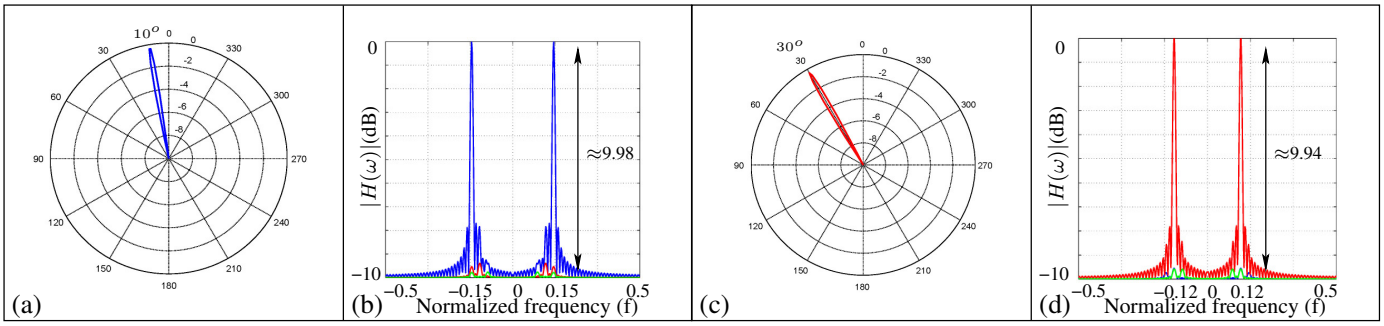

Fig. 7. a) Array pattern of the 2-D IIR SBP filter tuned for a DOA ψ_1, where $\psi_1 = 10^o$; b) 1-D frequency spectrum of the output of the 2-D IIR SBP obtained by selecting the spatial frequencies ω'_{x_1}, for the given temporal frequency ω'_{ct} for $\psi_1 = 10^o$; c) Array pattern of the 2-D IIR SBP filter tuned for a DOA ψ_2, where $\psi_2 = 30^o$; d) 1-D frequency spectrum of the output of the 2-D IIR SBP obtained by selecting the spatial frequencies ω'_{x_2}, for the given temporal frequency ω'_{ct} for $\psi_2 = 30^o$.

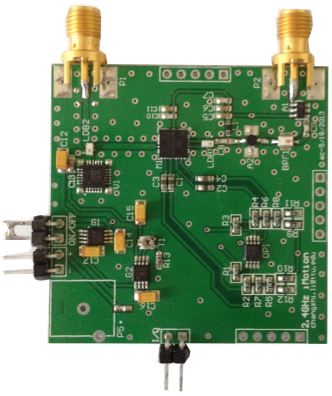

Fig. 8. Doppler radar element designed at the PCB level [3].

array of mixers, our digital signal processing and sampling process occurs at a manageably low frequency, and is simply determined by the maximum doppler shift that can be expected in the radar. For example, for carrier frequencies in the 2-3 GHz range, for speeds less than 100 mph, the Doppler shifts are in the kilo Hertz range, which in turn, allows the ADC converters and digital processing algorithms for directional beamforming and velocity detection to run at slow speeds. The low bandwidth of the digital processing algorithms allow low-end processors such as low cost microcontrollers and embedded systems to achieve the RF sensing required without relying on high-end digital solutions which can be expensive for radar target applications. For purposes of illustration, we considered a scenario where the SBP filter is tuned to capture signals at 10^o. The input signal-to-interference ratio (SIR) was ≈ -7.27 dB. Fig. 5(c) shows the frequency response of the 2-D IIR SBP filter when tuned to a DOA of 10^o. The 2-D frequency spectrum of the filtered output is shown in Fig. 5(d), where and it can be seen that the filtered output comprises only of the PW that has a DOA of 10^o, while the other two waves have been suppressed. The output side SIR was computed to be 4.19 dB, which shows the high directional selectivity of the 2-D IIR SBP filter, with an SIR improvement of about 11.46 dB. Further more we have investigated the array patterns for the DOA's under interest. Fig. 7 (a),(c) illustrate the array patterns of the 2-D IIR SBP for DOA's of 10^o and 30^o and it could be clearly seen that at each instance main beam of the polar pattern is in the direction of the desired DOA. Fig. 7 (b),(d) indicate the 1-D frequency spectrum of the filtered output for the two DOA's and the plot shows the frequencies of other plane waves being suppressed while the frequency shift corresponding to the plane wave of interest being preserved.

Because the temporal frequency of the output signal is proportional to the frequency shift Δf we can therefore obtain velocity and range profiles using (2) and (3), respectively. Similarly, since the spatial frequency ω_x used in the spatial bandpass filter corresponds to the DOA of the wave, we can extract the DOA. With the knowledge of velocity and angle of arrival we can accurately sense targets in the 2-D space which can act as an input to the central controlling unit of CPS including AVs.

V. Conclusion

A novel architecture was proposed to obtain the speed and angular details of scatterers surrounding the radar targets under consideration. The doppler radars used enable us to isolate distinct scatterers from surrounding clutter, and obtain the information about their velocity profiles based on the frequency shift between the transmitted and recieved signals. The 2-D IIR SBP filter was used to extract the directional properties of the scatterer. The 2-D SBP filters are generally used to selectively enhance desired signals of interest at intermediate frequency, based on their DOA. In this study, the received signals, upon downconversion using the transmitted signal, is subject to the 2-D SBP filter after down-sampling.

The proposed algorithm was verified by considering three scatterers moving at speeds of 31 ms,$^{-1}$ 18 ms^{-1} and 27 ms^{-1}, respectively, from the ULA of receiver antennas at 10,^{o} 30,^{o} 60^o along the broadside array direction. The received 2-D signal is downconverted by mixing it with the transmitted signal, resulting in the ROS occupying the shifted frequency points. This frequency shift was used to estimate the speed of the scatterers. The downconverted signals were further downsampled and made subject to the 2-D IIR SBP filter, where the DOA of the received signal was estimated to determine the angular location of the scatterer. The simulation was carried out on MATLAB, and the results demonstrated effective directional sensing of individual scatterers, distinctly.

Acknowledgements

Dr Madanayake thanks US National Science Foundation (NSF) awards EARS - 1247940 and EECS - 1408361.

REFERENCES

[1] A. Kandil, A. Wagner, A. Gotta, and E. Badreddin, "Collision avoidance in a recursive nested behaviour control structure for unmanned aerial vehicles," in *IEEE International Conference on Systems Man and Cybernetics (SMC)*, pp. 4276–4281, October 2010.

[2] M. Lange and J. Detlefsen, "94 GHz three-dimensional imaging radar sensor for autonomous vehicles," *IEEE Transactions on Microwave Theory and Techniques*, vol. 39, pp. 819–827, May 1991.

[3] C. Gu, R. Li, H. Zhang, A. Y. Fung, C. Torres, S. B. Jiang, and C. Li, "Accurate respiration measurement using DC-coupled continuous-wave radar sensor for motion-adaptive cancer radiotherapy," *IEEE Transactions on Biomedical Engineering*, vol. 59, no. 11, pp. 3117–3123, 2012.

[4] C. Gu, G. Wang, Y. Li, T. Inoue, and C. Li, "A hybrid radar-camera sensing system with phase compensation for random body movement cancellation in doppler vital sign detection," *IEEE Transactions on Microwave Theory and Techniques*, vol. 61, pp. 4678–4688, December 2013.

[5] M. Mercuri, P. Soh, G. Pandey, P. Karsmakers, G. Vandenbosch, P. Leroux, and D. Schreurs, "Analysis of an indoor biomedical radar-based system for health monitoring," *IEEE Transactions on Microwave Theory and Techniques*, vol. 61, pp. 2061–2068, May 2013.

[6] A. Droitcour, O. Boric-Lubecke, V. Lubecke, and J. Lin, "0.25 – μm CMOS and BiCMOS single-chip direct-conversion doppler radars for remote sensing of vital signs," in *IEEE International Solid-State Circuits Conference*, vol. 1, pp. 348–349, February 2002.

[7] Y. Wang, Q. Liu, and A. E. Fathy, "CW and pulse–doppler radar processing based on FPGA for human sensing applications," *IEEE Transactions on Geoscience and Remote Sensing*, vol. 51, pp. 3097–3107, May 2013.

[8] Y. Kim and H. Ling, "Through-wall human tracking with multiple doppler sensors using an artificial neural network," *IEEE Transactions on Antennas and Propagation*, vol. 57, pp. 2116–2122, July 2009.

[9] S. Y. Kim and G. M. Rebeiz, "A low-power BiCMOS 4-element phased array receiver for 76–84 GHz radars and communication systems," *IEEE Journal of Solid-State Circuits*, vol. 47, pp. 359–367, February 2012.

[10] C. Fulton and W. J. Chappell, "Calibration of a digital phased array for polarimetric radar," in *IEEE MTT-S International Microwave Symposium Digest (MTT)*, pp. 161–164, May 2010.

[11] T. Snow, C. Fulton, and W. J. Chappell, "Transmit–receive duplexing using digital beamforming system to cancel self-interference," *IEEE Transactions on Microwave Theory and Techniques*, vol. 59, pp. 3494–3503, December 2011.

[12] W. J. Chappell and C. Fulton, "Digital array radar panel development," in *IEEE International Symposium on Phased Array Systems and Technology (ARRAY)*, pp. 50–60, October 2010.

[13] C. Wijenayake, A. Madanayake, and L. T. Bruton, "Broadband multiple cone-beam 3-D IIR digital filters applied to planar dense aperture arrays," *IEEE Transactions on Antennas and Propagation*, vol. 60, pp. 5136–5146, November 2012.

[14] R. M. Joshi, A. Madanayake, J. Adikari, and L. T. Bruton, "Synthesis and array processor realization of a 2-D IIR beam filter for wireless applications," *IEEE Transactions on Very Large Scale Integration (VLSI) Systems*, vol. 20, pp. 2241–2254, December 2012.

[15] R. Joshi, A. Madanayake, L. Bruton, and M. Maini, "Discrete-space continuous-time analog circuits for spatially-bandpass 2-D IIR beam filters," in *7th International Workshop on Multidimensional Systems*, pp. 1–7, September 2011.

[16] A. Madanayake, C. Wijenayake, R. Joshi, M. Almalkawi, L. Belostotski, L. Bruton, and V. Devabhaktuni, "Electronically scanned RF-to-bits beam aperture arrays using 2-D IIR spatially bandpass digital filters," *Multidimensional Systems and Signal Processing*, vol. 25, no. 2, pp. 313–335, 2014.

[17] R. Fletcher and J. Han, "Low-cost differential front-end for doppler radar vital sign monitoring," in *Microwave Symposium Digest, 2009. MTT '09. IEEE MTT-S International*, pp. 1325–1328, June 2009.

[18] L. Lu, C. Gu, C. Li, and J. Lin, "Doppler radar noncontact vital sign monitoring," in *Neural Computation, Neural Devices, and Neural Prosthesis* (Z. Yang, ed.), pp. 41–62, Springer New York, 2014.

[19] G. Wang, J.-M. Munoz-Ferreras, C. Gu, C. Li, and R. Gomez-Garcia, "Application of linear-frequency-modulated continuous-wave (LFMCW) radars for tracking of vital signs," *IEEE Transactions on Microwave Theory and Techniques*, vol. 62, pp. 1387–1399, June 2014.

[20] A. Madanayake, *Real-time FPGA Architectures for Space-time Frequency-planar MDSP*. PhD thesis, University of Calgary, April 2008.

[21] H. Madanayake and L. Bruton, "A speed-optimized systolic array processor architecture for spatio-temporal 2-D IIR broadband beam filters," *IEEE Transactions on Circuits and Systems I: Regular Papers*, vol. 55, pp. 1953–1966, August 2008.

[22] L. Bruton and N. Bartley, "Three-dimensional image processing using the concept of network resonance," *IEEE Transactions on Circuits and Systems*, vol. 32, pp. 664–672, July 1985.

[23] P. Agathoklis and L. T. Bruton, "Practical-BIBO stability of N-dimensional discrete systems," *IEEE Proceedings of Electronic Circuits and Systems*, vol. 130, pp. 236 –242, December 1983.

[24] A. Madanayake, C. Wijenayake, R. Joshi, M. Almalkawi, L. Belostotski, L. Bruton, and V. Devabhaktuni, "Electronically scanned RF-to-bits beam aperture arrays using 2-D IIR spatially bandpass digital filters," *Multidimensional Systems and Signal Processing*, vol. 25, no. 2, pp. 313–335, 2014.

[25] A. Sengupta, A. Madanayake, R. Gómez-García, and E. D. Engeberg, "Wideband aperture array using RF channelizers and massively-parallel digital 2D IIR filterbank," in *SPIE Defense+ Security*, pp. 90771G–90771G, International Society for Optics and Photonics, 2014.